JACS
JOURNAL OF THE AMERICAN CHEMICAL SOCIETY

Communication

pubs.acs.org/JACS

Time-Resolved Detection of Surface Oxide Formation at Individual Gold Nanoparticles: Role in Electrocatalysis and New Approach for Sizing by Electrochemical Impacts

Cameron L. Bentley, Minkyung Kang, and Patrick R. Unwin*

Department of Chemistry, University of Warwick, Coventry CV4 7AL, United Kingdom

Supporting Information

ABSTRACT: Nanoparticle (NP) impacts on electrode surfaces has become an important method for analyzing the properties and activity of individual NPs, by either (i) electrocatalytic reactions or (ii) volumetric (dissolution) analyses. Using Au NPs as an exemplar system, this contribution shows that it is possible to detect surface oxide formation at individual NPs, which can occur on a rapid time scale (few μs). The charge associated with this "surface oxidation method" can be used for sizing (with results that are comparable to TEM) despite charges of only fC being measured. This platform further allows the role of surface oxides in electrocatalysis to be elucidated, with the time scale of oxide formation being controllable (i.e., "tunable") via the applied potential, as illustrated through studies of borohydride and hydrazine electro-oxidation. Finally, all of these studies are carried out on an oxide-covered Au substrate, which can be prepared and regenerated straightforwardly on an Au electrode, through the applied potential.

Single nanoparticle (NP) measurements are a new frontier in electrochemistry.[1] Although experimentally challenging, such measurements bring considerable advantages compared to those on ensembles of NPs on support electrodes, where the response is averaged over many NPs and complicated by the effects of surface coverage, NP distribution and NP-support interactions.[2] Among a limited range of methods, single nanoparticle electrochemical impacts (SNEI) is becoming increasingly popular for detecting and analyzing individual NPs. This typically involves monitoring the current−time (I−t) transients associated with the stochastic collision of NPs from a (dilute) colloidal solution with a collector electrode, with the detected current arising from either (i) a heterogeneous electron-transfer reaction taking place at the NP surface (e.g., electrocatalytic amplification[3−6]) or (ii) the electro-dissolution of the NP itself.[7,8]

In this contribution, we introduce a third approach to investigate the dynamic interaction between metal NPs and a collector electrode, in which the detected current arises from NP surface oxidation, as is shown schematically in Figure 1a for the case of an Au NP. This measurement is much more challenging than the (volumetric) anodic oxidation of metal NPs,[7,8] due to the smaller charges involved and much faster time scale of the process, but opens up new prospects for detecting noble metals and analyzing the formation of surface oxides, which can greatly influence (retard or accelerate) electrocatalysis.[9] Figure 1a highlights a further innovation of our work, which is the use of the same material (Au) for the collector electrode as the NPs, with the activity/passivity of the collector electrode controlled through the applied potential. Usually, the potential applied at the Au collector electrode will be sufficiently positive to form gold oxide (i.e., AuO_x), and therefore when Au NPs freely diffusing in solution sporadically make contact with the collector electrode, a small oxidation current "blip" is expected due to the formation of AuO_x on the NP surface.[10] A thin layer of AuO_x on the Au collector electrode (Figure 1b) makes it electrochemically inert (i.e., "passivated") toward certain reactions, such as the oxidation of borohydride and hydrazine, considered herein. By maintaining the electrode at a potential where the oxide is stable, individual collisions of Au NPs are detectable through electrocatalytic amplification (Figure 1c) which competes with NP deactivation through oxide formation. The resulting oxidation I−t ("blip") response thus informs on the electrocatalytic process at a NP surface while undergoing passivation. This will be larger in magnitude than that obtained in the absence of the electroactive species (e.g., Figure 1d).

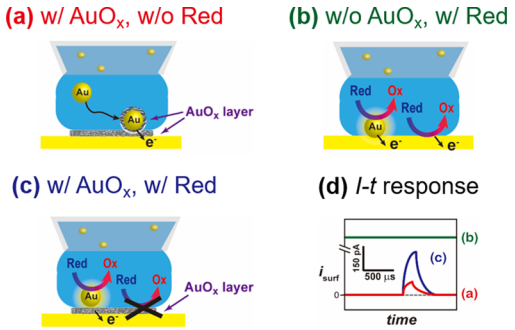

Figure 1. Schematic of a single NP collision event at an Au collector electrode surface that is (a) passive (i.e., w/AuO_x), with no redox species present in solution (i.e., w/o Red); (b) active (i.e., w/o AuO_x), with redox species present in solution (i.e., w/Red); and (c) passive, with redox species present in solution. The I−t response expected for the NP landing events shown in panels a, b and c are shown in panel d as red, green and blue traces, respectively.

The experimental setup employed in this study is shown schematically in Figure S1a and is based on scanning electrochemical cell microscopy (SECCM),[11] which has previously

Received: August 4, 2016
Published: September 9, 2016

DOI: 10.1021/jacs.6b08124
J. Am. Chem. Soc. 2016, 138, 12755−12758

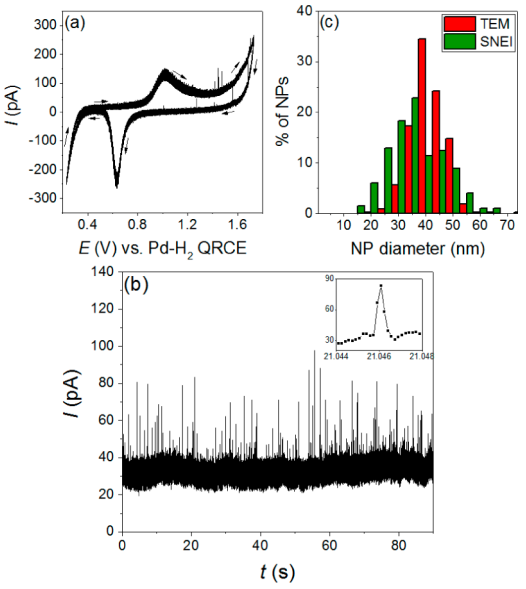

Figure 2. (a) A CV (ν = 100 mV s^{-1}) obtained in a solution containing 20 mM NaOH and 44 pM Au NPs at an Au collector electrode formed by meniscus contact with a 7 ± 1 μm diameter micropipette. The arrows indicate the direction of the voltammetric sweep. (b) I–t trace at 1.6 V (vs Pd–H_2 QRCE) in a solution containing 20 mM NaOH and 44 pM Au NPs. Inset is a zoomed in view of a "typical" landing event, taking place at 21.046 s. (c) Normalized NP diameter distributions from TEM (red bars, N = 479) and analysis of the charge passed (green bars, N = 202) during landing events under the conditions outlined in panel b.

been shown to be advantageous in many applications, notably SNEI,[12−14] due to flexibility of electrode size (determined by the area of meniscus contact) and material, as well as greatly enhanced signal/noise compared to alternative configurations.[2] In this approach, a microdroplet electrochemical cell is formed through contact of the meniscus that protrudes from the end of a tapered micropipette (Figure S1b,c) with a polycrystalline Au surface. The diameter of the cell ("droplet") is comparable to the diameter of the probe (i.e., 7 ± 1 μm, Figure S1d). Note that in this work, we used a single-channel pipette, rather than a dual-channel (θ) pipette used previously.[13,14] The citrate capped Au NPs for the landing experiments were synthesized using a literature procedure[15] (representative TEM image shown in Figure S2a) and had an average diameter of 39 ± 6 nm (histogram of size distribution shown in Figure S2b).

We first consider the detection of Au NPs through the current arising from NP surface oxidation, as shown schematically in Figure 1a. A cyclic voltammogram (CV) at an Au collector electrode in a solution containing 20 mM NaOH and 44 pM Au NPs is shown in Figure 2a. The CV starts at a potential of 0.6 V (all potentials are against a Pd–H_2 quasi-reference counter electrode, QRCE), and AuO_x formation and corresponding stripping (reduction) peaks at the collector electrode can be seen at potentials of 1.1 and 0.7 V on the forward and reverse sweeps, respectively. Moreover, at potentials beyond the AuO_x formation peak on the outgoing scan, but prior to the stripping peak on the reverse sweep, a series of transient current spikes (or "blips") ranging in size from 10 to 80 pA are evident. These are attributable to the (surface) oxidation of Au NPs in solution, which sporadically make contact with the collector electrode in the potential region where it is passivated (oxidized).

To investigate the dynamic interaction between Au NPs and the Au collector electrode in further detail, an I–t trace was recorded at an applied potential of 1.6 V, with typical results shown in Figure 2b. Evidently, a series of short I–t transients ("blips") similar to those shown in Figure 2a are detected. The experimental landing frequency (ca. 1 Hz) is comparable to that predicted[3,14] for the diffusion-limited flux of NPs to the collector electrode surface in this experimental configuration (ca. 0.8 Hz). The inset in Figure 2b is a zoomed in view of a "typical" NP landing event; AuO_x formation occurs on a very rapid time scale at this potential, with a typical "event" lasting ca. 500 μs. Evidently, the detection of the rapid I–t transients associated with AuO_x formation requires high time resolution (data acquisition rate = 165 μs/point, with each point being the average of 33 readings of 5 μs intervals), as well as an excellent signal-to-noise (S/N) ratio (<20 pA peak-to-peak background current). Note that this time scale is convoluted to some extent by the electrometer response and data acquisition rate. We show below that when the AuO_x formation process is set in competition with electrocatalysis, one can obtain an even better estimate of the AuO_x formation time scale.

It is reasonable to consider that the charge (Q) passed during each landing event (i.e., from integrating the I–t transients) is proportional to the surface area of the reacting NP (surface oxidation). Calculating the diameter of a NP from Q requires knowledge of (i) the oxidation state of the Au in AuO_x, (ii) surface atom density, which is lattice plane dependent and (iii) the shape of the NPs. In aqueous alkaline media and at the potential investigated (i.e., 1.6 V vs Pd–H_2 QRCE), bulk Au is expected to undergo a $2e^-$ oxidation to form a monolayer of $Au(OH)_2$ and/or AuO.[10] By assuming that the Au NPs are spherical and the same oxidation mechanism also applies to the NP surface (i.e., n = 2 and monolayer AuO_x coverage), and taking the surface atom density of Au in the NPs to be 10^{15} atoms cm^{-2} [calculated for the (100) plane of a fcc crystal with a lattice constant of 4.07 Å], a NP size distribution was constructed from Q, as shown in Figure 2c. The shape of the distribution is in good agreement with the one constructed by TEM image analysis (also shown in Figure 2c), with the main difference being that the histogram constructed by Q is broader (mean diameter = 39 ± 10 nm) than from TEM (mean diameter =39 ± 6 nm). The smallest NP diameter measurable under the conditions shown in Figure 2 (limited by the S/N) would ca. 17 nm. There may be scope for improving this in the future. Overall, the concurrence between the two histograms shown in Figure 2c highlights the capability of this new "surface oxidation method" (see Figure 1a) for NP sizing analysis. This is particularly important because, as mentioned above, a number of noble metals are not easily oxidized but do form oxides and, further, this is a nondestructive analysis method (the surface oxidation could be reversed if needed). In addition, using this method, there may be scope for extracting information on the kinetics of oxide formation at the single NP level in future studies.

The next experimental setup investigated is shown schematically in Figure 1b,c, using borohydride oxidation as the "model" electrocatalytic process (e.g., Red = $[BH_4]^-$). A CV obtained on an Au collector electrode in a 20 mM NaOH solution containing 2.0 mM $NaBH_4$ is shown in Figure 3a. On Au electrodes, borohydride undergoes the following complicated, $8e^-$ oxidation to produce borate (BO_2^-) and H_2O in alkaline media:[16,17]

$$BH_4^- + 8OH^- \rightarrow BO_2^- + 6H_2O + 8e^- \quad (1)$$

In Figure 3a, on the forward sweep, starting from a potential of 0.13 V, the current rapidly rises to a "plateau" (ca. 4 nA), which spans the potential region 0.5 to 1.1 V, before rapidly decreasing

DOI: 10.1021/jacs.6b08124
J. Am. Chem. Soc. 2016, 138, 12755−12758

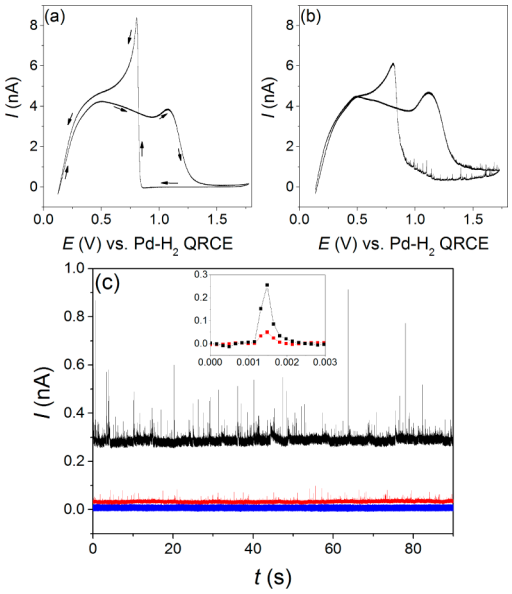

Figure 3. CVs (ν = 100 mV s^{-1}) obtained from the oxidation of 2.0 mM $[BH_4]^-$ (from $NaBH_4$) in a solution containing 20 mM NaOH and (a) 0 pM or (b) 44 pM Au NPs at an Au collector electrode formed by meniscus contact with a 7 ± 1 μm diameter micropipette. (c) I–t curves obtained at a applied potential of 1.6 V (vs Pd–H_2 QRCE) in solutions containing 20 mM NaOH together with 2.0 mM $[BH_4]^-$ (blue trace); 44 pM Au NPs (red trace); 2.0 mM $[BH_4]^-$ + 44 pM NPs (black trace). Inset is a zoomed in view of "typical" landing events obtained in the presence and absence of $[BH_4]^-$, taking place at 47.318 and 21.046 s, respectively.

to approximately zero, due to surface deactivation ("passivation"). On the reverse sweep, the Au surface remains inactive until a potential of ca. 0.8 V, where the current rapidly rises and peaks at ca. 8 nA, before dropping back down to the "plateau" value of 4 nA, and then retracing the voltammetric behavior from the forward sweep. The abrupt deactivation (ca. 1.1 V) and activation (ca. 0.8 V) of the Au electrode coincide with the formation and stripping of AuO_x, respectively (Figure 2a), demonstrating the strong electrode-surface dependence of the $[BH_4]^-$ oxidation process. Taking into account that the diffusional flux in SECCM and related droplet-based techniques (e.g., Figure S1a) is ca. 13% of that for the same sized disc electrode,[11] and assuming that the number of electrons transferred is 8 (eq 1) and the diffusion coefficient of $[BH_4]^-$ in alkaline media is 1.6×10^{-5} cm^2 s^{-1},[16] a steady-state limiting current of 4.5 ± 0.6 nA is expected from a droplet diameter of 7 ± 1 μm, which is in excellent agreement with that observed experimentally in Figure 3a, suggesting that the $[BH_4]^-$ oxidation process can attain mass-transport control. It should be noted that the CV obtained at an Au substrate with the microdroplet cell setup qualitatively resembles that obtained at a similarly sized Au ultramicroelectrode (UME, shown in Figure S3), except that the measured current (and hence diffusional flux) at the UME is approximately 10 times larger, as expected.[11,14]

Shown in Figure 3b is a CV obtained under the conditions outlined above, but with the addition of Au NPs (44 pM). The shape of the CV is very similar to that of Figure 3a, except for a series of current transients ("blips") that are present in the region where the Au collector electrode is passive on both the anodic and cathodic scans (schematic shown in Figure 1c). The increased size of the current spikes (50 to 600 pA) relative to when no $[BH_4]^-$ is present (10 to 80 pA, Figure 2) indicates that they must arise from both borohydride oxidation and oxide formation, as discussed below.

Shown in Figure 3c are I–t traces obtained at a collector electrode potential of 1.6 V in the presence or absence of $[BH_4]^-$ and Au NPs. In the presence of $[BH_4]^-$ and absence of Au NPs (blue trace), a miniscule, constant current of ca. 10 pA is observed, indicating that the oxide-covered Au substrate is not particularly active toward borohydride oxidation, consistent with Figure 3a. As discussed above (Figure 2c), in the absence of $[BH_4]^-$, but in the presence of Au NPs (red trace), current "blips" ranging in size from 10 to 80 pA (superimposed on a background current of ca. 30 pA) are observed, which arise from the surface oxidation of impacting NPs. In the presence of both $[BH_4]^-$ and Au NPs (black trace), much larger current "blips" ranging in size from 25 to 600 pA (superimposed on a background current of ca. 300 pA) are observed. Inset is a zoomed in view of a "typical" landing event in the presence or absence of borohydride: the current transient is of a similar duration (ca. 500 μs), because the reaction in both cases is shut off when the NP is surface-oxidized. The charge passed in the presence of $[BH_4]^-$ (93 fC) is about 5 times higher than in its absence (18 fC), again, due to both borohydride oxidation and oxide formation. Subtracting the average charge from oxide formation (16 fC) from the total charge passed in this feature gives an estimate of the charge passed due to borohydride oxidation (77 fC), and assuming the full $8e^-$ process takes place at the NP surface, this corresponds to the oxidation of just ca. 100 zmol of $[BH_4]^-$ during the event shown in the inset of Figure 3c.

In a number of previous studies,[3,17,18] it has been highlighted that it is often impossible to distinguish whether a current "blip" response arises due to a nonsticking interaction between the NP and collector electrode (e.g., Kang et al.[14]) or due to deactivation of the NP after it "sticks" on the collector electrode surface (e.g., Robinson et al.[19]). In the present study, at the applied potential (1.6 V) it has been confirmed that the NPs deactivate rapidly upon landing (Figure 2), and given that the NPs and the collector electrode are made from the same material (Au), there is a very high probability that the current "blip" response is due to a "sticking interaction" followed by rapid deactivation. This is consistent with the experimentally measured landing frequency (*vide supra*) and is further confirmed by changing the applied potential. As shown in Figure S4, at an applied potential of 1.2 V, the current transients decay on a much slower time scale (milliseconds to seconds) because of the slower rate of surface oxidation of the Au NP. But the longer duration indicates that the NPs must remain in contact with the collector electrode surface. As a consequence, the charge passed during each landing event in the presence of $[BH_4]^-$ is much larger at this collector electrode potential (e.g., ca. 8 pC in the inset of Figure S4). In effect, the shape and characteristics of the current–time transients (i.e., the time scale of NP deactivation) can be "tuned" by controlling the potential applied at the collector electrode.

A histogram showing the distribution of the peak currents obtained at 1.6 V in the presence of both $[BH_4]^-$ and Au NPs is shown in Figure S5. Although a few "large" current transients (i.e., >400 pA) were observed, the majority are smaller than 100 pA (mean peak current is 81 pA). This is much smaller than the diffusion-controlled steady-state current ($i_{ss} \approx 400$ pA) predicted for a 39 nm diameter NP on a surface, calculable from[2]

$$i_{ss} = 4\pi(\ln 2)nFDCr_{NP} \quad (2)$$

where n is the number of electrons transferred, F is Faraday's constant, D and C are the diffusion coefficient and bulk

DOI: 10.1021/jacs.6b08124
J. Am. Chem. Soc. 2016, 138, 12755–12758

concentration of $[BH_4]^-$ and r_{NP} is the radius of the NP. A steady-state electrocatalytic current would expected to be established rapidly (governed by the characteristic steady-state diffusion time, $\approx r^2_{NP}/D \approx 0.3\ \mu s$). The fact that a peak current is observed that is greatly attenuated (about 20% of that expected) means that deactivation (AuO_x formation) occurs on a comparable time scale (few microseconds), a small fraction of the electrometer time constant,[13] at 1.6 V.

The few landing events that produced peak currents that are larger than predicted by eq 2 are thought to arise from NP aggregates, which form as a result of the addition of $NaBH_4$/NaOH. NP aggregation is increasingly recognized as important in NP impact studies.[8,19,20] This was confirmed by performing dynamic light scattering (DLS, see the inset of Figure S6), where the average size of the NPs (aggregates) increased continuously with time, after mixing. Furthermore, the influence of aggregation on the SNEI experiments was investigated by performing a measurement 1 h after solution preparation; as shown in Figure S6, the observed current spikes are, on average, much larger than those seen in Figure 3c, which was recorded in a "fresh" solution.

In a final set of experiments, the setup outlined in Figure 1b,c was used with Red = hydrazine. A CV obtained on an Au substrate in a 20 mM NaOH solution containing 2.0 mM $[N_2H_5][HSO_4]$ is shown in Figure S7a. Hydrazine undergoes the following $4e^-$ oxidation to produce N_2 and H_2O in alkaline media:[21]

$$N_2H_4 + 4OH^- \rightarrow N_2 + 4H_2O + 4e^- \quad (3)$$

The shape and characteristics of the CV are discussed in detail in the Supporting Information. Shown in Figure S7b is a CV obtained under the same conditions outlined above, except in the presence of 44 pM of Au NPs. Again, the shape of the CV is very similar to that obtained in the absence of Au NPs (Figure S7a), except a series of current transients ("blips") are observed in the region where the Au collector electrode is not active (i.e., 1.7 to 0.65 V on the reverse sweep only). The inset of Figure S7b is an $I-t$ trace obtained at a hold potential of 1.1 V after taking the potential to 1.75 V; $I-t$ transients ranging in size from 50 to 300 pA (200 pA expected from eq 2), which typically decay on a 10 to 100 ms time scale are observed under these conditions. Again, the observed "blip" response is attributable to the deactivation of the Au NP by surface oxidation, as discussed above.

In conclusion, the landing of Au NPs on an (oxidized) Au surface have been detected electrochemically with high time resolution, either through the direct oxidation of the NP surface or electrocatalytic amplification, using the oxidation of borohydride and hydrazine as illustrative examples. Au NP surface oxidation occurs on a rapid timescale (potential dependent, and as short as a few μs), but can be detected with high precision, and the charge associated with this process can be used to estimate the NP surface area, demonstrating the possibility of the "surface oxidation method" for NP size analysis. With electrocatalytic amplification in this setup, it is possible to assess the impact of surface oxide formation on electrocatalysis, with the time scale of deactivation being controllable through the collector electrode potential. Finally, NP impact studies have tended to use a dissimilar (more inert) collector electrode material compared to the NP, but this study has shown that Au NPs can be detected on an Au electrode, with the surface oxidation state (passivity) carefully tuned via the applied potential.

■ ASSOCIATED CONTENT

Supporting Information

The Supporting Information is available free of charge on the ACS Publications website at DOI: 10.1021/jacs.6b08124.

Full experimental details, CVs obtained at UMEs and additional NP landing experiments in the presence of $[BH_4]^-$ or hydrazine (PDF)

■ AUTHOR INFORMATION

Corresponding Author

*P.R.Unwin@warwick.ac.uk

Notes

The authors declare no competing financial interest.

■ ACKNOWLEDGMENTS

C.L.B. acknowledges the Australian Government's Endeavour Fellowship Programme. M.K. acknowledges support from the University of Warwick Chancellor's International Scholarship.

■ REFERENCES

(1) Oja, S. M.; Fan, Y.; Armstrong, C. M.; Defnet, P.; Zhang, B. *Anal. Chem.* **2016**, *88*, 414.
(2) Kleijn, S. E. F.; Lai, S. C. S.; Koper, M. T. M.; Unwin, P. R. *Angew. Chem., Int. Ed.* **2014**, *53*, 3558.
(3) Xiao, X. Y.; Bard, A. J. *J. Am. Chem. Soc.* **2007**, *129*, 9610.
(4) Xiao, X. Y.; Fan, F. R. F.; Zhou, J. P.; Bard, A. J. *J. Am. Chem. Soc.* **2008**, *130*, 16669.
(5) Dasari, R.; Robinson, D. A.; Stevenson, K. J. *J. Am. Chem. Soc.* **2013**, *135*, 570.
(6) Hill, C. M.; Kim, J.; Bard, A. J. *J. Am. Chem. Soc.* **2015**, *137*, 11321.
(7) Krause, K. J.; Yakushenko, A.; Wolfrum, B. *Anal. Chem.* **2015**, *87*, 7321.
(8) Brasiliense, V.; Patel, A. N.; Martinez-Marrades, A.; Shi, J.; Chen, Y.; Combellas, C.; Tessier, G.; Kanoufi, F. *J. Am. Chem. Soc.* **2016**, *138*, 3478.
(9) Rodriguez, P.; Koper, M. T. M. *Phys. Chem. Chem. Phys.* **2014**, *16*, 13583.
(10) Tremiliosi-Filho, G.; Dall'Antonia, L. H.; Jerkiewicz, G. *J. Electroanal. Chem.* **1997**, *422*, 149.
(11) Snowden, M. E.; Güell, A. G.; Lai, S. C. S.; McKelvey, K.; Ebejer, N.; O'Connell, M. A.; Colburn, A. W.; Unwin, P. R. *Anal. Chem.* **2012**, *84*, 2483.
(12) Kleijn, S. E. F.; Lai, S. C. S.; Miller, T. S.; Yanson, A. I.; Koper, M. T. M.; Unwin, P. R. *J. Am. Chem. Soc.* **2012**, *134*, 18558.
(13) Chen, C. H.; Ravenhill, E. R.; Momotenko, D.; Kim, Y. R.; Lai, S. C. S.; Unwin, P. R. *Langmuir* **2015**, *31*, 11932.
(14) Kang, M.; Perry, D.; Kim, Y.-R.; Colburn, A. W.; Lazenby, R. A.; Unwin, P. R. *J. Am. Chem. Soc.* **2015**, *137*, 10902.
(15) Haiss, W.; Thanh, N. T. K.; Aveyard, J.; Fernig, D. G. *Anal. Chem.* **2007**, *79*, 4215.
(16) Mirkin, M. V.; Yang, H. J.; Bard, A. J. *J. Electrochem. Soc.* **1992**, *139*, 2212.
(17) Zhou, H. J.; Fan, F. R. F.; Bard, A. J. *J. Phys. Chem. Lett.* **2010**, *1*, 2671.
(18) Jung, A. R.; Lee, S.; Joo, J. W.; Shin, C.; Bae, H.; Moon, S. G.; Kwon, S. J. *J. Am. Chem. Soc.* **2015**, *137*, 1762.
(19) Robinson, D. A.; Kondajji, A.; Castaneda, A. D.; Dasari, R.; Crooks, R. M.; Stevenson, K. J. *J. Phys. Chem. Lett.* **2016**, *7*, 2512.
(20) Kleijn, S. E. F.; Serrano-Bou, B.; Yanson, A. I.; Koper, M. T. M. *Langmuir* **2013**, *29*, 2054.
(21) Chen, C.-H.; Jacobse, L.; McKelvey, K.; Lai, S. C. S.; Koper, M. T. M.; Unwin, P. R. *Anal. Chem.* **2015**, *87*, 5782.

DOI: 10.1021/jacs.6b08124
J. Am. Chem. Soc. 2016, 138, 12755−12758